JOURNAL OF MATERIALS SCIENCE 28 (1993) 2607–2614

Anodic behaviour and passivation of a lead electrode in sodium carbonate solutions

E. E. ABD EL AAL* S. ABD EL WANEES
Chemistry Department, Faculty of Science, United Arab Emirates University, Al-Ain, P. O. Box 17551, United Arab Emirates

A. ABD EL AAL
Chemistry Department, Faculty of Science, Zagazig University, Zagazig, Egypt

Cyclic voltammograms of a lead electrode were obtained in Na_2CO_3 solution as a function of the starting potential, electrolyte concentration and voltage scanning rate. The shape of the voltammograms was found to depend on the starting potential as well as the sweep number. This is probably due to changes in the activation state of the electrode surface. The first anodic portion of the voltammograms is characterized by a shoulder and two peaks corresponding to the formation of $PbCO_3$, PbO and PbO_2, respectively. The cathodic portion shows the occurrence of two peaks corresponding to the reduction of PbO_2 to PbO and PbO to Pb, successively, followed by the formation of PbH_2. An increase in concentration of CO_3^{2-} ions leads to a negative shift in the values of the peak potentials, E_p, accompanying the formation of PbO and PbO_2. In addition, the current density for both the anodic oxidation peaks showed marked dependence on the concentration of the electrolyte. An increase in the scanning rate was observed to lead an increase in the size of the voltammograms. The current density of both the anodic peaks and the anodic passivation region were proportional to $v^{1/2}$. Such behaviour is expected in a diffusion-controlled processes. In addition, the anodic peaks are shifted towards more positive values of potential, whereas the cathodic peaks are shifted in the negative direction, indicating irreversible formation of the passive film on the electrode surface.

1. Introduction

The electrochemical behaviour of lead in carbonate media has attracted attention because the major part of the early work was performed galvanostatically and the results were poorly resolved [1, 2]. To date no information has been reported in the literature regarding the interpretation of the cyclic voltammograms (CVs) of lead in carbonate media.

The present paper is concerned with the study of the electrochemical behaviour of lead in Na_2CO_3 solution employing the cyclic voltammetric technique. The influence of starting potential, carbonate concentration, and scanning rate were examined. The implications of these results with reference to the mechanisms of the reaction involved, is discussed.

2. Experimental procedure

Spectroscopically pure lead (Johnson–Matthey, UK) was used as the test material throughout the present work in the form of short rods, 0.98 mm diameter. These rods were fixed to Pyrex glass tubes with Araldite so that the total exposed surface area was 0.75 cm^2. Electrical contact was achieved through thick copper wires soldered to the end of the rods, not exposed to the solution. Before being used, the electrodes were abraded, successively, with 0-, 00- and 000- grade emery papers, then degreased with acetone and finally washed with doubly-distilled water (which was also used in preparing the electrolytes of Na_2CO_3).

A two-compartment cell was used for obtaining the CVs. The counter electrode was a platinum wire. Its compartment was separated from the working electrode (main) compartment by means of a G_4 centred glass disc. The potential of the working electrode was measured relative to a saturated calomel electrode (SCE) using a salt bridge, whose tip was almost touching the electrode surface.

The potential of the working electrode was controlled by a Wenking laboratory Potentiostat (LB75). A voltage scan generator (VSG72, Wenking) was used to provide a linearly increasing or deceasing control voltage input to the potentiostat. The CVs were recorded using an X–Y recorder-type Linseis LY.21 (Cole Parmer Instruments, USA). Each experiment

*Author to whom all correspondence should be addressed.

0022–2461

was performed on a newly polished electrode and with freshly prepared electrolyte. The temperature was adjusted to 25 ± 0.2 °C using an air thermostat.

3. Results and discussion

3.1. Effect of starting potential

Fig. 1 shows the curves of three different CVs starting from the quasi-steady state potential ($E = -0.7$ V SCE), in 1×10^{-1} mol l^{-1} Na_2CO_3 solution at a sweep rate 25 mV s^{-1}. The first curve represents the first sweep, the second and third sweeps are also illustrated. It is obvious that the forward and backward sweeps are different. This could be an indication of an irreversible process. Dissimilarities between successive sweeps can be attributed to different initial states of the electrode surface. After the first sweep, the electrode surface is thought to be covered partially by the oxidation products that have not been reduced. Therefore, the second and third sweeps are quite different, as would be expected. The initial state of the electrode determines, to a large extent, the shape of the resulting CVs, as can be seen by inspection of the curves of Figs 2–4. In these figures, the electrode was polarized cathodically at −1.2, −1.6 and −2.1 V, respectively, for 10 min before starting the CVs. In all cases, the behaviour demonstrated by the CVs is quite different from that in Fig. 1.

The results of Figs 1–4, are a clear indication that the initial state of the electrode surface seems to be an important factor regarding the shape of the current–potential curves. The interesting point here is that if polarization started at the open-circuit potential (−0.7 V (SCE)), the electrode might have been covered with a pre-immersion oxide film, Fig. 1. This would possibly arise from atmospheric oxidation of the metal surface or from corrosion taking place at the designated open-circuit potential [3]. Undoubtedly, the resulting CVs will be a function of these different starting conditions. However, Fig. 4 illustrates that hydrogen evolution ensues at a starting potential of −2.1 V (SCE). In this case, the oxide film on the electrode surface can be reduced [4], and a reproducible initial state of the electrode surface is consequently achieved. Thus, comparison of the different results requires prior knowledge of the starting conditions [3, 5–7].

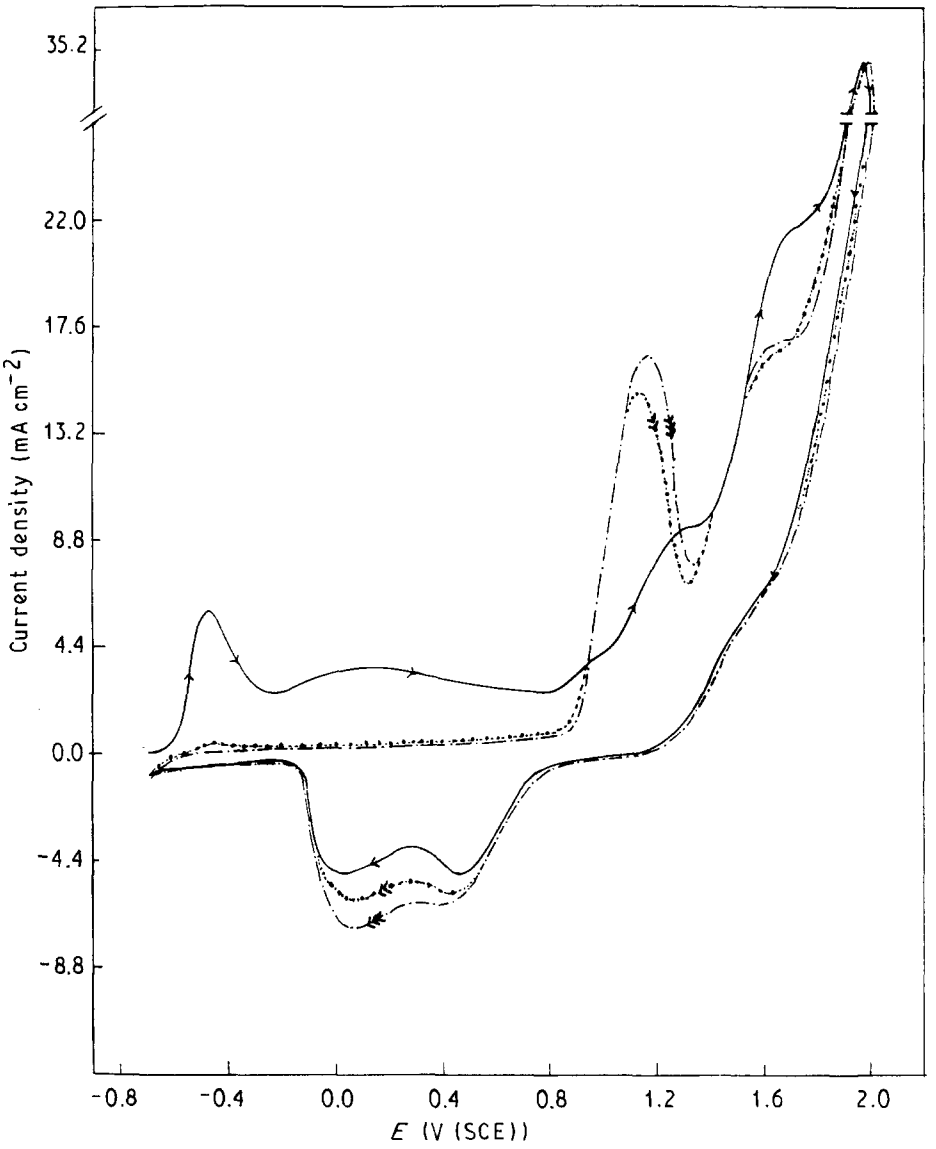

Figure 1 Scanning voltammograms of the lead electrode in 1×10^{-1} mol l^{-1} Na_2CO_3 starting from the open-circuit potential, −0.7 V (SCE), at a rate of 25 mV s^{-1}. Sweep: (—) 1, (. . . .) 2, (-.-) 3.

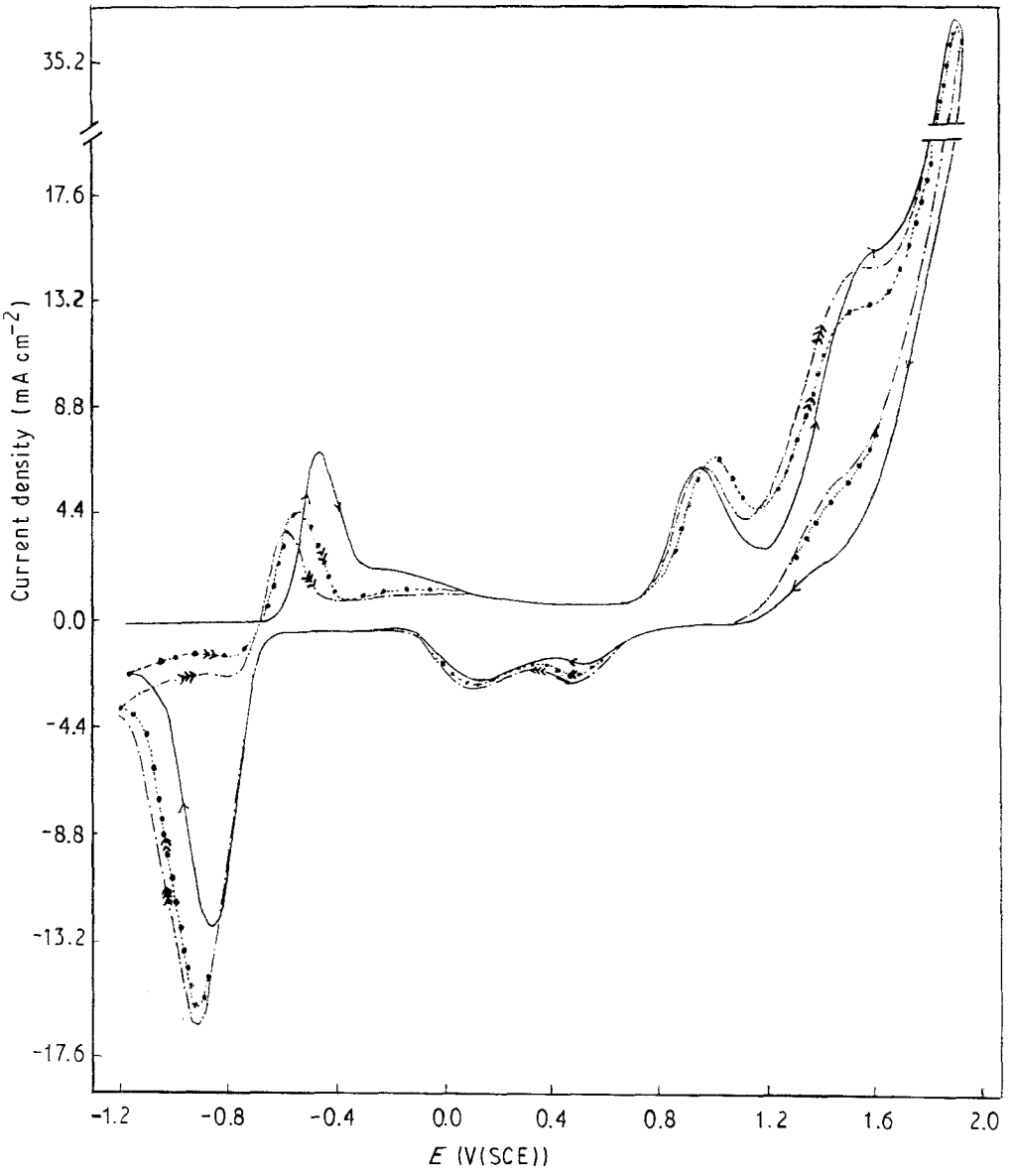

Figure 2 Scanning voltammograms of the lead electrode in 1×10^{-1} mol l^{-1} Na_2CO_3, prepolarized for 10 min at -1.2 V (SCE), at a rate of 25 mV s^{-1}. For key, see Fig. 1.

In Fig. 4, the CVs reported between -2.1 and $+1.9$ V (SCE) exhibit several regions which change during reported cycles. In the first anodic half cycle, two major peaks (II, IV) and a shoulder, I, have been observed, Peak II is recorded at -0.52 V which is preceded by Shoulder I at -0.7 V. This shoulder is found to disappear after the first cycle. Also, the stable passive region, III, is observed to extend to about 0.62 V. Peak IV is recorded at about 0.86 V. The transpassive plateau are found to start around 1.1 V (Region V). In the vicinity of 1.5 V, the contribution of the oxygen evolution current is also manifested. During the cathodic half cycle, Peaks VI, VII, IX appeared at about 0.34, -0.88 and -1.6 V, respectively. Peak VI is a composite one that could plausibly correspond to either a competing or a step-wise process that will be explored in detail later.

Correlation between the experimentally observed maxima and the possible electrode processes taking place can be achieved. The data in Fig. 4, reveal that the first anodic portion of the CVs has the same general characteristics as those reported in galvanostatic measurement for pure lead [2, 8] and lead alloys [1] in Na_2CO_3 solutions. The anodic portion of the CVs is characterized by the presence of Shoulder I prior to the first major anodic peak, II. The potential of the Pb/PbO electrode at pH 11.1 (1×10^{-1} mol l^{-1} Na_2CO_3) was calculated [4] to be -0.54 V (SCE). It is observed, however, that the anodic oxidation of lead in sodium carbonate solution commences at -0.7 V (SCE), Fig. 4. It is more likely that the first phase to be formed is a lead carbonate salt. Similar conclusions were reached by Khairy *et al.* [1] and by us [8], on the basis of data obtained from the galvanostatic oxidation in Na_2CO_3 solutions. Therefore, one might assume that Shoulder I corresponds to the formation of $PbCO_3$ on the electrode surface according to [1, 2, 8].

$$Pb + CO_3^{2-} \rightarrow PbCO_3 + 2e^- \quad (1)$$

This shoulder is followed by a sharp current rise leading to the first major anodic peak, II. The peak potential recorded at -0.52 V (SCE) nearly coincides with the calculated [4] value for the Pb/PbO potential

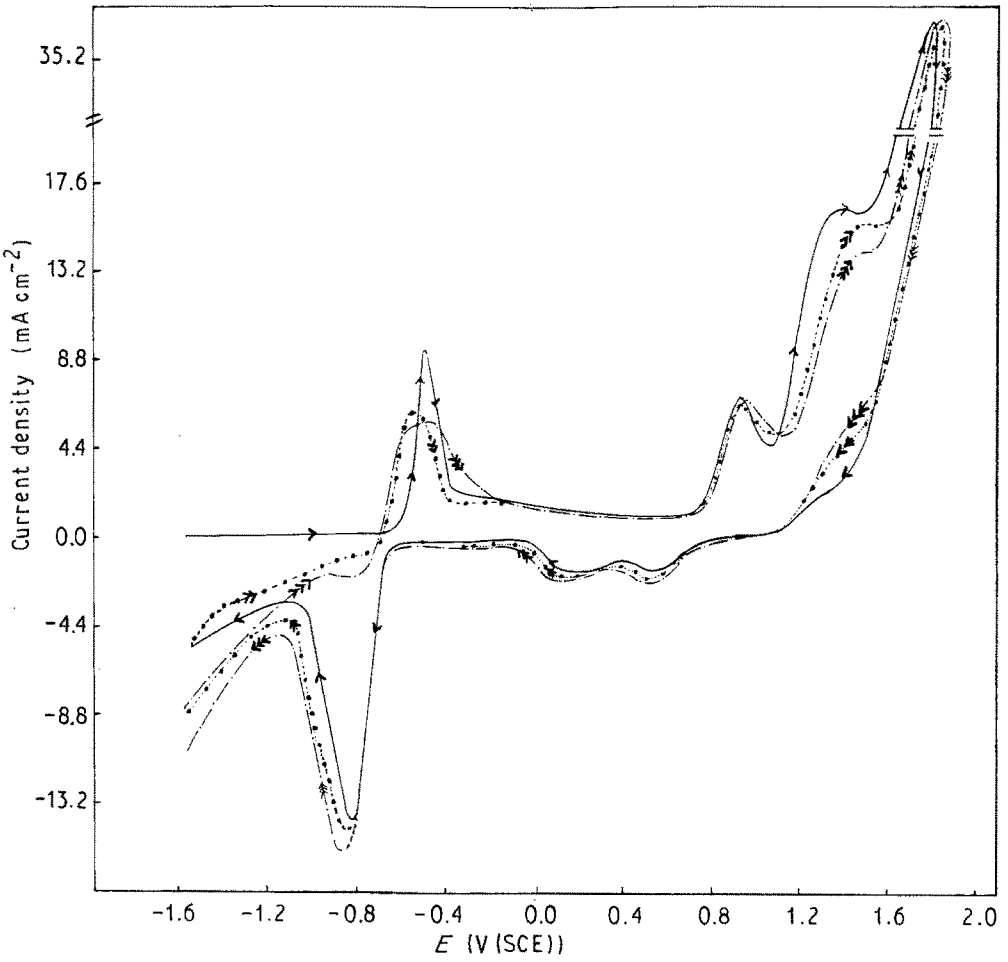

Figure 3 Scanning voltammograms of the lead electrode in 1×10^{-1} mol l^{-1} Na_2CO_3, prepolarized for 10 min at -1.6 V (SCE), at a rate of 25 mV s^{-1}. For key, see Fig. 1.

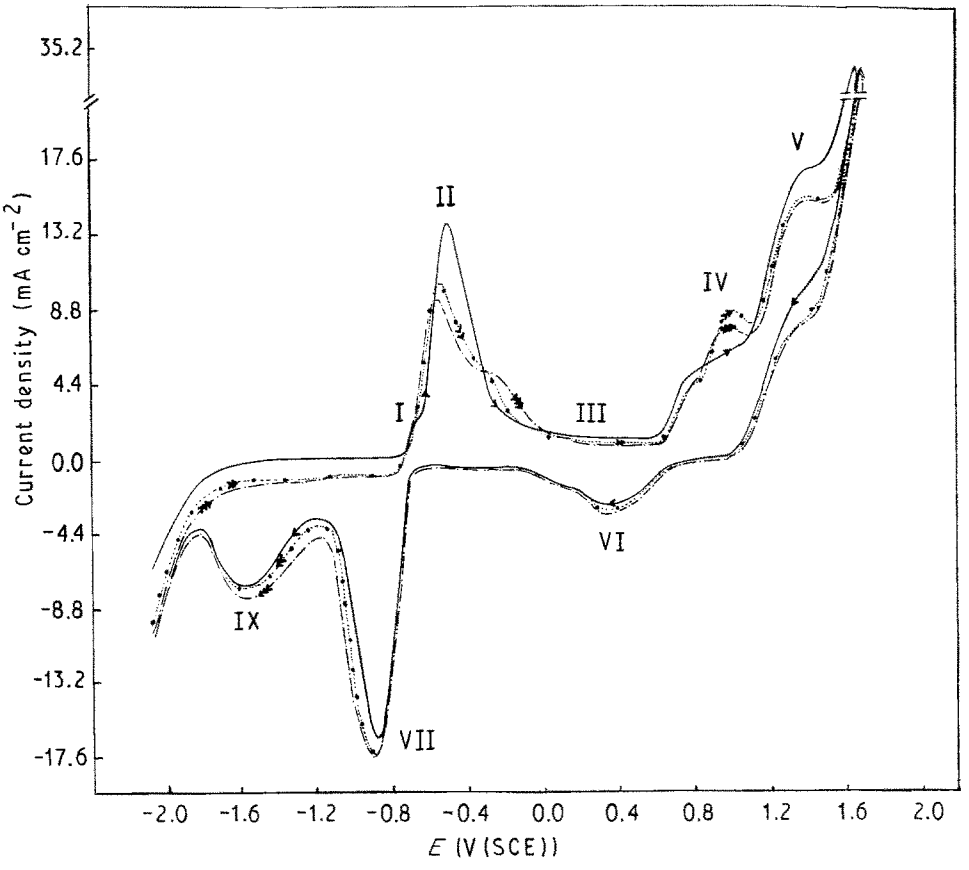

Figure 4 Scanning voltammograms of the lead electrode in 1×10^{-1} mol l^{-1} Na_2CO_3, prepolarized for 10 min at -2.1 V (SCE), at a rate of 25 mV s^{-1}. For key, see Fig. 1.

(as reported above). Hence, one might conclude that PbO is formed in this potential range. Khairy *et al.* [1], reported that formation of PbO may be attributed to the transformation of $PbCO_3$ to oxide and/or the direct oxidation of lead in the available pores of lead carbonate. Alternatively, one may argue that the process of oxide formation, under prevailing experimental conditions could be explained on mechanistic grounds as [9–12]

$$Pb + OH^- \rightleftharpoons (PbOH)_{ads} + e^- \quad (2)$$

$$(PbOH)_{ads} + OH^- \rightleftharpoons Pb(OH)_2 + e^- \quad (3)$$

$$Pb(OH)_2 \rightleftharpoons PbO + H_2O \quad (4)$$

After Peak II, the electrode becomes passive and the current density decreases to lower value (Region III) and extends over a wide potential range. The passive current density, i_{III}, increases quite slowly as the potential shifts to more positive values. This increase may plausibly be due to the establishment of a new process on the electrode surface that is likely to be the transformation of PbO into PbO_2 [12, 13], in the region of Peak IV. The latter peak, which is the second major one, had been previously observed in Na_2CO_3 solution [1, 8] and had been attributed to the transformation of PbO to PbO_2 through the reaction between hydroxyl ion and the PbO formed on the surface, to give Pb_3O_4 and then PbO_2, according to

$$3PbO + 2OH^- \rightarrow Pb_3O_4 + H_2O + 2e^- \quad (5)$$

$$Pb_3O_4 + 4OH^- \rightarrow 3PbO_2 + 2H_2O + 4e^- \quad (6)$$

After Peak IV, the current rises again to give a transpassive plateau, V, followed by a sudden increase in current density. This region might correspond to the dissolution of some PbO_2 to form plumbate ions [4]. The sudden increase in the current is due to oxygen evolution

$$4OH^- \rightarrow O_2 + 2H_2O + 4e^- \quad (7)$$

The cathodic portion of the CVs in Fig. 4 shows three peaks (VI, VII and IX). The most positive peak, VI, appeared as a composite peak which is expected to occur in the region of PbO_2/Pb_3O_4 and Pb_3O_4/PbO potentials [1, 8], respectively. This could be explained on the grounds that PbO_2 will be reduced to Pb_3O_4 and the latter to PbO [14]

$$3PbO_2 + 2H_2O + 4e^- \rightarrow Pb_3O_4 + 4OH^- \quad (8)$$

$$5Pb_3O_4 + 11H_2O + 10e^- \rightarrow 3[5PbO \cdot 2H_2O] + 10OH^- \quad (9)$$

The second current peak, VII, occurred, approximately, in the region of the PbO/Pb potential [4] and hence it would correspond to the reduction of PbO to Pb [1, 8]. The most negative peak IX, can be attributed to the formation of PbH_2. Jones *et al.* [15] observed a similar reduction peak and attributed it to the hydride formation. This peak decreases as the concentration of carbonate increases. Such decreases can be interpreted in terms of the alkalinity of solution that leads to the depletion of hydrogen and hence hindrance of hydride formation [4, 8].

3.2. Effect of carbonate concentration

CVs were obtained for lead electrode in various solutions of Na_2CO_3 having a range of concentration between 5×10^{-2} and 1 mol l^{-1}. They were carried out between -2.1 and $+1.9$ V (SCE) at a scanning rate of 25 mV s^{-1}. The lead electrode was cathodically maintained at -2.1 V for 10 min in order to reduce oxides which are thought to form spontaneously on the metal surface prior to potential excursion.

As the carbonate concentration increased, the peak potential, E_p, of both Peaks II and IV were observed to shift towards more negative values with no significant effect on the shape of Shoulder I. The effect of reactant activity and of voltage scanning rate on the peak potential and peak current under conditions of semi-infinite linear diffusion serves as a diagnostic criterion frequently used for mechanistic studies [16, 18]. In reversible diffusion-limited reactions with soluble reactants and insoluble products under conditions of semi-infinite linear diffusion, E_p at room temperature is given by [17]

$$E_p = E^0 - 0.0218/n + (0.059/n) \log a_{CO_3^{2-}} \quad (10)$$

where n is the number of electrons involved in the reaction. Under such conditions, a plot of E_p versus $\log a_{CO_3^{2-}}$ is a straight line with a slope of 59 and 30 mV for one- and two-electron transfer reactions, respectively.

Fig. 5 shows plots of E_p versus log $a_{CO_3^{2-}}$ for both Peaks II and IV. The mean activity coefficient of Na_2CO_3 at different concentrations was calculated according to Moore [19]. Two straight lines were obtained having slopes of 30 and 38 mV for Peaks II and IV, in the same order. The value of 30 mV for the slope corresponding to Peak II, Fig. 5, is an indication that the current of this peak is supported by a two-electron transfer reaction whose overall reaction is likely to be [1, 8, 13]

$$Pb + 2OH^- \rightarrow PbO + H_2O + 2e^- \quad (11)$$

The value of 38 mV for the slope corresponding to Peak IV, Fig. 5, is somewhat larger than the theoretical value of 30 mV for a two-electron transfer reaction [20]. Such a value obtained might be explained in terms of a two-electron transfer reaction (Equation 12) and possibly a small proportion of a one-electron

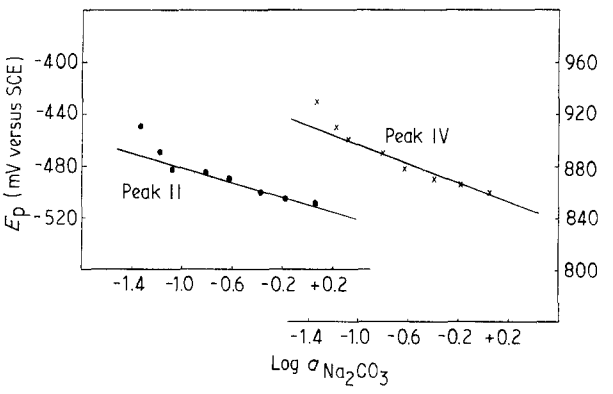

Figure 5 Relation between peak potential, E_p, and log $a_{Na_2CO_3}$ for Peaks II and IV.

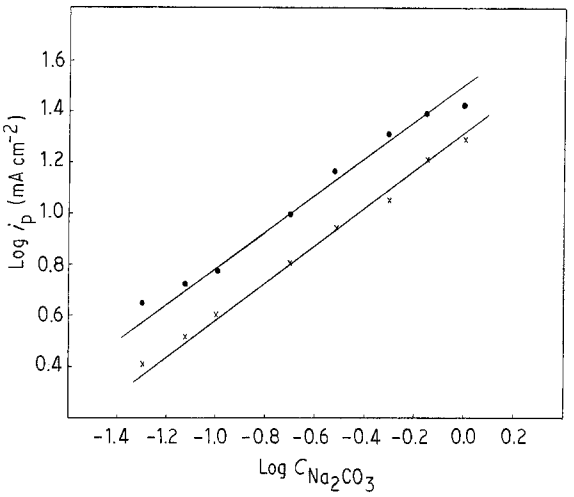

Figure 6 Variation of log i_p with the log concentration of Na_2CO_3 for Peaks (●) II and (×) IV.

transfer reaction owing to the formation of non-stoichiometric lead oxide (PbO_{1+x}, $x \simeq 0.57$) [21]. Thus, Peak IV may result from the following overall reaction [13]

$$PbO + 2OH^- \rightarrow PbO_2 + H_2O + 2e^- \quad (12)$$

The effect of voltage scanning rate and reactant concentration on the peak current, i_p, might also serve as another mechanistic criterion [17]. Thus, in reactions controlled by semi-infinite linear diffusion, the peak current is directly proportional to the reactant concentration and the square root of the voltage scanning rate, v, i.e.

$$i_p \propto v^{1/2} C^0 \quad (13)$$

Fig. 6 shows plots of log i_p versus log carbonate concentration for both Peaks II and IV. It is clear that

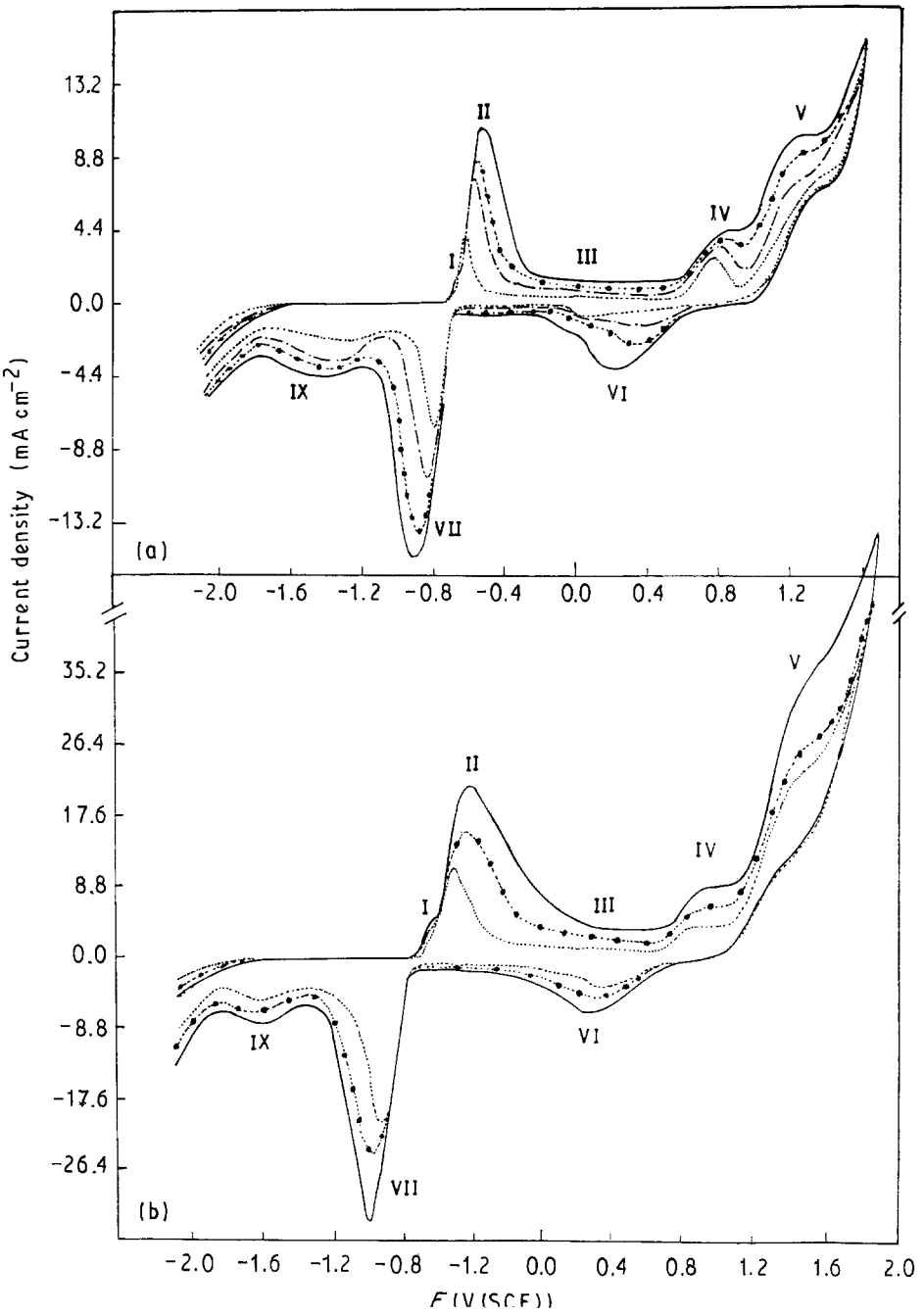

Figure 7 Effect of voltage scanning rates on CVs of lead in 1×10^{-1} mol l^{-1} Na_2CO_3. (a) (- - -) 5 mV s^{-1}, (— · —) 15 mV s^{-1}, (- - · - -) 25 mV s^{-1}, (—) 35 mV s^{-1}. (b) (. . .) 50 mV s^{-1}, (- - · - -) 75 mV s^{-1}, (—) 100 mV s^{-1}.

the data are well represented by two straight lines, within experimental error, over a large range of concentrations satisfying the equation

$$\log i_p = a + b \log C_{CO_3^{2-}} \quad (14)$$

where a and b are constants. Furthermore, the value of b is about 0.75, well within the expected value of 1 for a diffusional process [17].

3.3. Effect of voltage scanning rate

The effect of increased voltage scanning rate is illustrated in Fig. 7. The CVs were obtained for a lead electrode in Na_2CO_3 solution having a concentration of 1×10^{-1} mol l^{-1}. The figure reveals that an increase in the sweep rate, v, leads to increase in the size of the CVs, except that a slight change for Shoulder I is observed.

As the sweep rate increases, the anodic peaks are shifted towards more positive values of potential, whereas the cathodic peaks are shifted in the negative direction. It has been established that the greater separation between anodic and cathodic peaks, the corresponding processes, would be the irreversible formation of a passive film on the electrode surface [22].

The influence of sweep rate on the current density along Peak II, passive Region III and Peak IV, is shown in Fig. 8. The relation between i_{II} and $v^{1/2}$ is represented by a straight line that goes through the origin. This is a clear indication that the anodic dissolution along this peak is a diffusion-controlled process [23]. The authors had previously suggested that such a process is limited by diffusion of soluble Pb^{2+} ions away from the electrode surface [8].

The lack of linearity between i_{III} and $v^{1/2}$ at 400 mV (in the passive region) represented in Fig. 8, might be attributed to the competing processes of formation of PbO_2 from PbO and dissolution of the latter [8, 23].

With regard to Peak IV, a linear relationship between i_{IV} and $v^{1/2}$ is observed with a small intercept in Fig. 8. In this connection it has been suggested that the presence of an intercept indicates that the rate-determining step in the formation of PbO_2 is not a single diffusion-controlled process [22]. Such processes might be diffusion of soluble species formed from the reaction between PbO_2 and hydroxide ions away from the electrode, whereas the hydroxide ions present in the electrolyte diffuses towards the electrode–solution interface.

A comparison of the quantity of charge under the anodic and cathodic peaks is a useful method for detecting the formation of soluble reaction products [20]. In Fig. 9, the change of the ratio Q_a/Q_c with the scanning rate, v, for the lead electrode in 1×10^{-1} mol l^{-1} Na_2CO_3 is depicted. The quantity of electricity was integrated between -1.2 and $+1.4$ V (SCE) in order to exclude the charge involved in both lead hydride and oxygen evolution at the two extremes of the CVs. The ratio Q_a/Q_c increases steadily until it approaches a plateau value of 1.9 at higher sweep rates. Such an observation might be due to dissolution processes [22]. At lower sweep rates, the

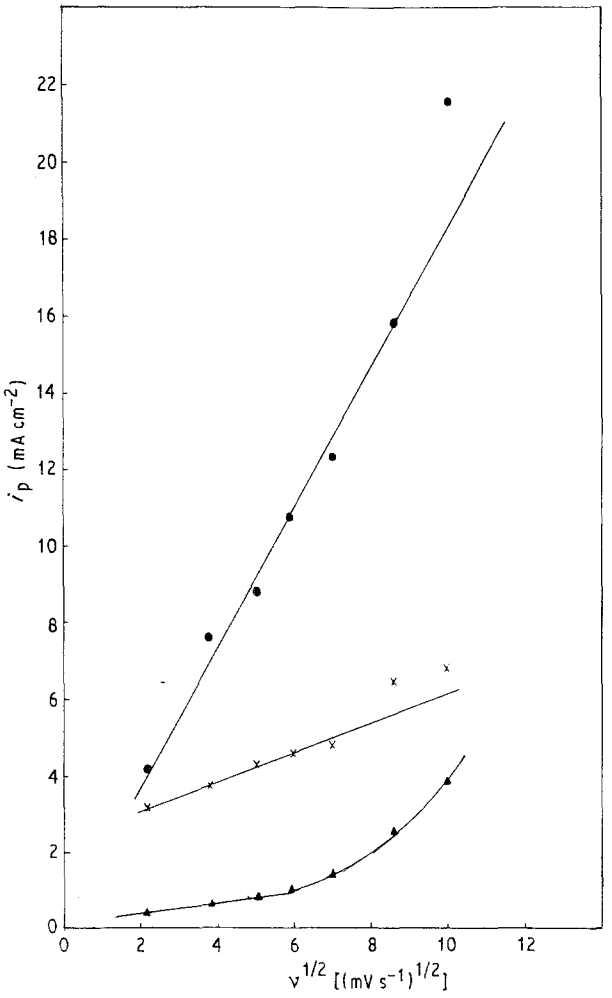

Figure 8 Dependence of peak current density along (●) Peak II, (▲) passive Region III and (×) Peak IV on the square root of sweep rate in 1×10^{-1} mol l^{-1} Na_2CO_3.

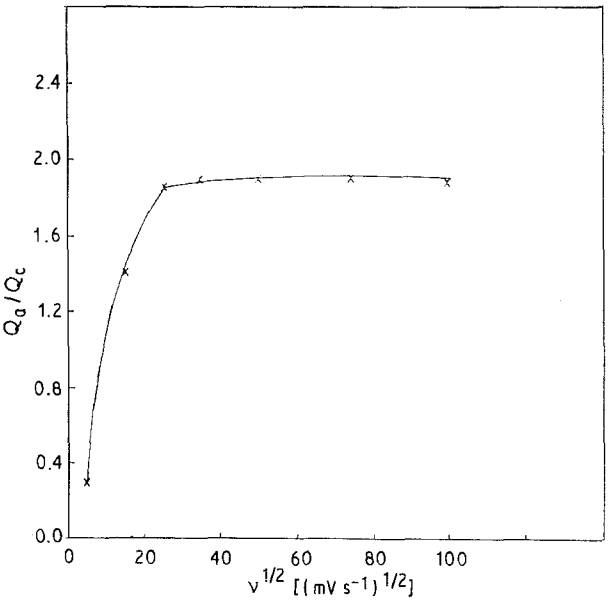

Figure 9 Anodic to cathodic charge ratios as a function of sweep rate in 1×10^{-1} mol l^{-1} Na_2CO_3.

dissolution products formed during the anodic sweep have sufficient time to diffuse into the bulk of the solution before being reduced on reversing the sweep [24]. In addition, the ratio $Q_a/Q_c > 1$ at a higher sweep rate indicates that the major part of the anodic

charge is used to produce soluble species [20, 22]. The anodic soluble reaction produced, namely the biplumbite ion $HPbO_2^-$, might result from an electrochemical reaction [8, 12, 13]

$$Pb + 3OH^- \rightleftharpoons HPbO_2^- + H_2O + 2e^- \quad (15)$$

and/or from PbO through a chemical reaction

$$PbO + OH^- \rightleftharpoons HPbO_2^- \quad (16)$$

It is noteworthy here that the dissolution of some PbO_2 as the plumbate ion PbO_3 could also be considered as a plausible explanation.

References

1. E. M. KHAIRY, A. A. ABDUL AZIM and K. M. EL SOBKI, *J. Electroanal. Chem.* **11** (1966) 282.
2. A. A. ABDUL AZIM and M. M. ANWAR, *Corros. Sci.* **9** (1969) 245.
3. S. M. ABD EL HALEEM and A. ABD EL AAL, *Corros. Prevent. Cont.* **29** (1982) 13.
4. M. POURBAIX, "Atlas of Electrochemical Equilibria" (Pergamon press, Oxford, 1966).
5. S. M. ABD EL HALEEM, E. E. ABD EL AAL, A. A. ABD EL FATTAH and A. ABD EL AAL, *Res Mech.* **17**, (1986) 179.
6. R. D. ARMSTRONG and I. BAURHOO, *J. Electroanal., Chem. Interfacl. Electrochem.* **34** (1972) 41.
7. D. D. MACDONALD and D. OVEN, *J. Electrochem. Soc.* **120** (1973) 317.
8. E. E. ABD EL AAL, *Bull. Soc. Chem. Fr.*, **128** (1991) 351.
9. S. ABD EL WANEES, E. E. ABD EL AAL and A. ABD EL AAL *Anti Corros. Meth and Mat.* **28** (1991) 4.
10. V. I. BIRSS and M. T. SHEVALIER, *J. Electrochem. Soc.* **134** (1987) 802.
11. *Idem, ibid.* **134** (1987) 1594.
12. *Idem, ibid.* **137** (1990) 2643.
13. A. A. ABDUL AZIM and K. M. EL SOBKI, *Corros. Sci.* **12** (1972) 207.
14. P. RUETSCHI and R. T. ANGSTADT, *J. Electrochem. Soc.* **111** (1964) 1323.
15. P. JONES, H. R. THIRSK and W. F. K. WYNNE-JONES, *Trans. Farad. Soc.* **52** (1956) 1003.
16. R. BATES, "Electrometric pH Measurements" (John Wiley, New York, 1954) p. 41.
17. P. DELEHAY, "New Instrumental Methods in Electrochemistry" (Interscience, New York, 1954) Ch.6.
18. R. ADAMS, "Electrochemistry at Solid Electrodes" (Marcel Dekker, New York, 1969) p. 143.
19. W. J. MOORE, "Physical Chemistry" (Longman, London, 1978) p. 443.
20. S. M. ABD EL HALEEM and B. G. ATEYA, *J. Electroanal. Chem.* **117** (1981) 309.
21. J. S. BUCHANAN, N. P. FREESTONE and L. M. PETER, *ibid.* **182** (1985) 383.
22. H. DO DUC and P. TISSOT, *Corros. Sci.* **19** (1979) 179.
23. S. S. ABD EL REHIM, A. M. ABD EL HALIM and E. E. FOAD, *Surf. Technol.* **18** (1983) 313.
24. V. I. BIRSS and W. WAUDO, *Can. J. Chem.* **67** (1989) 1098.

Received 24 April 1991
and accepted 14 August 1992